Available online at www.sciencedirect.com
ScienceDirect
Journal of Sound and Vibration 308 (2007) 831–844
JOURNAL OF SOUND AND VIBRATION
www.elsevier.com/locate/jsvi

Set-oriented numerical analysis of a vibro-impact drilling system with several contact interfaces

Nicolai Neumann*, Thomas Sattel

Heinz Nixdorf Institute, Fuerstenallee 11, 33102 Paderborn, Germany

Accepted 28 March 2007
The peer review of this article was organised by the Guest Editor
Available online 14 June 2007

Abstract

The dynamics of a novel piezoelectric device for drilling of brittle materials is investigated. This device consists of a resonantly driven piezoelectric actuator, a drill stem, as well as a free-flying mass oscillating and impacting between the tip of the piezoelectric actuator and the end of the drill stem. Contact interfaces exist between the actuator and the mass, the mass and the drill stem as well as between the drill stem and the machined material. Basic understanding of the device's dynamic behaviour is crucial, for example to enhance the drilling performance or to redesign the system for different corer or drill stem geometries. However, such a basic understanding is still missing. Experiments with a prototype device as well as simulations with simple models show irregular motion of the impacting mass. To investigate the complicated temporal behaviour of this system, so-called set-oriented numerical methods are applied. These methods are based on an adaptive subdivision technique for cell-mapping to approximate attractors and invariant measures. A model for the drilling device is proposed consisting of several degrees of freedom. The motion of the piezoelectric actuator tip follows a prescribed harmonic vibration; the free-flying mass is represented as a point mass. The drill stem is modelled as a rod structure to account for longitudinal wave propagation. The contact conditions between the different subsystems are described by complementary kinematics and force relations and Newton's impact law, respectively. Using the set-oriented methods, periodic and chaotic orbits are detected and parameter ranges for the occurrence of different types of solutions are determined. Additionally, basins of attraction for the corresponding attractors are computed. Information on the probability of attaining a particular attractor is obtained by quantifying its connected basin of attraction. An invariant measure is chosen which represents the drilling performance. For most important model parameters, for example the mass of the free-flying body or the actuator excitation frequency, drilling performance is evaluated by computing this invariant measure for each attractor. The computational results lead to a deeper understanding of the vibro-impact dynamics of this drilling device, reveal the global behaviour of the system dynamics and show the influence of different design parameters on the drilling performance.

*Corresponding author. Tel.: +49 525 160 6499; fax: +49 525 160 6278.
E-mail addresses: neumann@hni.upb.de, nicolaineumann@arcor.de (N. Neumann), sattel@hni.upb.de (T. Sattel).
URL: http://wwwhni.uni-paderborn.de/mud (N. Neumann), http://wwwhni.upb.de/mud/mitarbeiter/sattel (T. Sattel).

0022-460X/$ - see front matter © 2007 Elsevier Ltd. All rights reserved.
doi:10.1016/j.jsv.2007.03.076

1. A vibro-impact drilling system

The application under consideration is motivated by the so-called USDC—the Ultrasonic/Sonic Driller/Corer. The USDC is a new drilling device to work with brittle material such as rock or stone. Its idea and a prototype device were developed by Bar-Cohen et al. [1] as a tool for in situ rock sampling and analysis in support of the NASA planetary exploration program.

Fig. 1 shows the schematic set-up of the drilling device. One outstanding property of the USDC is its rather simple design—compared to normal hand-held drilling machines. This can be well asserted by Fig. 2: apart from the electrical driving unit, the drilling device consists of only three main parts, the piezoelectric actuator, the free-flying mass, and the drill stem.

The piezoelectric actuator—first of three parts of the device—is a longitudinal piezoelectric transducer with a stack of piezo-electric disc elements. These elements are excited by a harmonic voltage driving the actuator in its first longitudinal eigenmode and causing its tip to vibrate at an ultrasonic frequency of approximately 20 kHz. The actuator's body is not bounded in longitudinal direction: thus it is able to move (e.g. in a bouncing way) in its longitudinal direction with respect to the other parts of the drilling system. The second part is a mass of a few grams which bounces irregularly at *sonic* frequencies back and forth between the actuator's tip and the back of the drill stem. Its task is to transform *ultrasonic* low-amplitude vibrations of the piezoelectric actuator into sonic impulses of higher strength, which cause stress waves traveling in the drill stem. By its motion the free-mass maintains the necessary gap between the actuator and the drill stem. The drill stem as the third part guides the stress waves initiated by impacts with the free-mass towards the drill-bit/rock interface causing fracture in the rock.

The simple design of the USDC as well as promising experimental results and successful application for in situ rock sampling, see Bar-Cohen et al. [1], motivates approaches to investigate the application of this novel mechanism for example in hand-held drilling devices for drilling in concrete. Limitations of existing drilling technologies are the need for large axial preload and stall torques and a high power consumption. Those needs cannot be accommodated by lightweight robots and rovers. Their requirements motivated the development of the USDC system.

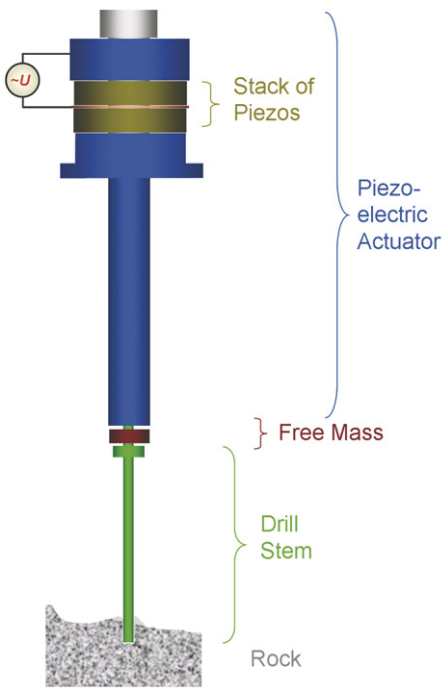

Fig. 1. Schematic set-up of the USDC.

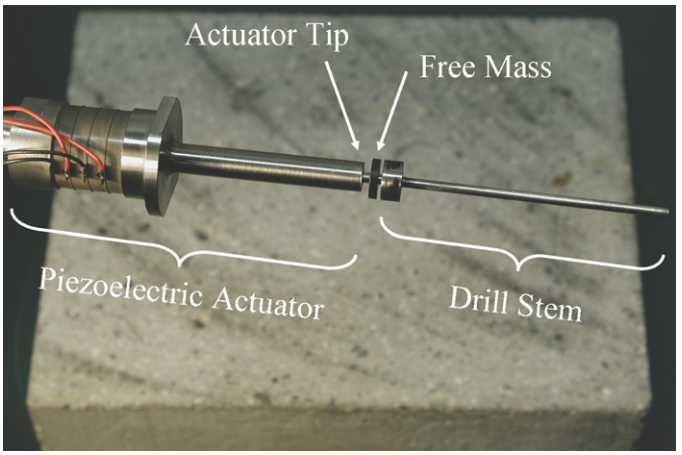

Fig. 2. Prototype of the Ultrasonic/Sonic Driller/Corer. The free mass which provides the focus of this paper's modelling task is visible in the centre.

Providing a new and promising drilling technology, the dynamic behaviour of the USDC system is, however, not understood in detail. It is for example unclear how the free-flying mass, the frequency, and the design of the drill stem influence the material removal rate. Even more, up to now it is unclear how this USDC device can be scaled up for applications with larger driller or corer, as they are needed in drilling of concrete. Also, the drilling speed must be significantly increased for applications on construction sites.

The key issue of the USDC device is the novel mechanism transfering ultrasonic vibrations of the piezoelectric actuator into larger vibrations of the free-flying mass. Thus, exploring the dynamics of this mechanism is essential for further developments with this drilling device. In Badescu et al. [2] finite element modelling and long-time integration of a simple spring-mass-model is chosen to analyse the dynamics of the contact-impact between the actuator and the free-flying mass. In Neumann et al. [3] and Neumann and Sattel [4] a different approach is chosen. Since experimental results show a complex dynamic behaviour of the vibrating mass, it is appropriate to perform a phase-space analysis in order to extract global information about the system dynamics. Information on the existence and domains of attraction of periodic orbits are sought, or statistical measures about the drilling performance based on the trajectories in the underlying phase space should be obtained. Therefore, so-called set-oriented methods are chosen for the model analysis, see e.g. Dellnitz and Junge [5]. These are new methods, based on the cell-mapping method by Hsu [6]. The methods analyse dynamical systems which can be represented by a set of difference equations. They use the *point mapping* technique which became well known from the work of H. Poincaré and G. Birkhoff—see also Babitsky [7, pp. 69–71].

The USDC device is modelled as a non-smooth system with vibro-impact behaviour. For such non-smooth systems approximate methods based on harmonic linearisation can be used, as given in Babitsky [7], in case the system behaviour in the interesting parameter range is time-periodic. Path following methods to analyse periodic non-smooth mechanical systems are presented by Leine and Nijmeijer [8]. All these methods cannot be applied for non-smooth systems with complex nonlinear dynamic behaviour. In Neumann et al. [3] and Neumann and Sattel [4] a simple one degree of freedom impact model is proposed for the model analysis. By describing the model as a time-discrete map the set-oriented methods could be applied. The analysis of this simple model reveals chaotic and periodic attractors and relative statistical measures about the performance of the energy transmission could be stated.

In this paper an extended model of the USDC vibro-impact dynamics is proposed, which includes the dynamics of the piezoelectric actuator. Focusing on the impacting free mass, Section 2 proposes a time discrete four-dimensional modelling approach for the non-smooth motion. In the proposed model the drill stem is simplified by a deflector at which the free mass rebounds. Energy dissipation during impacts is described by Newton's coefficient of restitution. Section 3 is dedicated to the analysis of the modelled system. In this section the set-oriented numerical method will be introduced and applied.

Finally, the paper is summarised and an outlook on future work is given in Section 4.

2. Time-discrete modelling of a vibro-impact system

2.1. The time-discrete dynamic system as map

Fig. 3 shows the three components of the simple model of the drill system, namely the piezoelectric actuator, called oscillator, the free mass, depicted as a ball, and the surface of the drill stem, denoted as deflector. The oscillator is excited in its first longitudinal eigenmode, as illustrated on the right-hand side in this figure. Thus, the lower end of the oscillator vibrates like a plunger in a harmonic manner with $\bar{u}(t) \coloneqq u_0 \cos \Omega t$. The displacements $x(t)$ of the oscillator's centre of gravity and $y(t)$ of the free mass are defined as height over the deflector.

The displacement $u(t)$ of the plunger can be formulated as harmonic excitation $\bar{u}(t)$ coupled to the oscillator motion $x(t)$:

$$u(t) = x(t) - \bar{u}(t). \tag{1}$$

A non-penetration contact condition

$$0 \leqslant y(t) \quad \forall t \quad \text{and} \quad y(t) \leqslant u(t) \quad \forall t \tag{2}$$

between the bodies is assumed in the modelling. A constant axial preload F_A is exerted to the oscillator to enhance the drilling performance. Gravity force acts on both bodies.

During operation of the drill system the ball gets in contact with either the plunger or the deflector between its free motion in the gap. Between two successive impacts both moving bodies perform forced motions due to gravity and the axial preload F_A. Their motions are completely defined by their corresponding initial value problems. Accordingly, giving the state variables at the time instant immediately *after* the impact with each other (ball–plunger contact) together with the corresponding phase information (with respect to the harmonic excitation) at which the impact occurs suffices to completely describe the motion of both moving bodies.

Hence, the dynamic state of the system is given only at those instants of time t_j at which an impact between ball and oscillator occurs (ball–plunger contact). Thus, the discrete state of the drill system is fully described

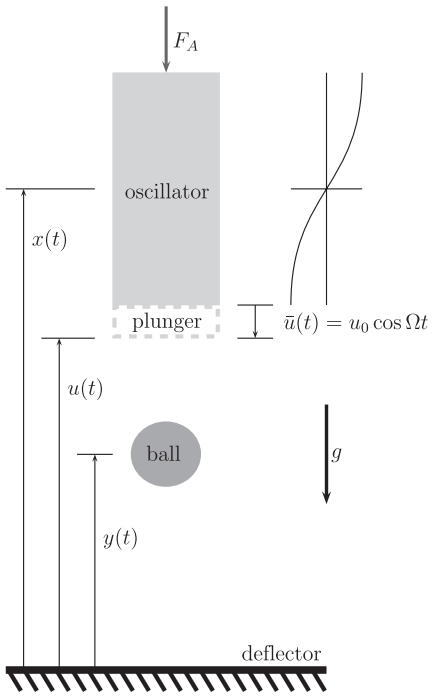

Fig. 3. Vibro-impact system model of degree four; the drill stem is described by a deflector.

by the state vector $\mathbf{x}(t_j) = [t_j, x(t_j), \dot{x}(t_j^+), \dot{y}(t_j^+)]^{\mathrm{T}}$, where the state variables are

t_j : time of impact;

$x(t_j)$: displacement of oscillator at time of impact;

$\dot{x}(t_j^+)$: velocity of oscillator immediately after the impact and

$\dot{y}(t_j^+)$: velocity of ball immediately after the impact.

Since the ball and the oscillator are in contact with each other during the time of impact, with $y(t_j) = u(t_j) = x(t_j) - \bar{u}(t_j)$ the displacement $y(t_j)$ of the ball during impact is simultaneously given. The abbreviating symbols

$$x_j \coloneqq x(t_j), \quad \dot{x}_j^+ \coloneqq \dot{x}(t_j^+), \quad \dot{y}_j^+ \coloneqq \dot{y}(t_j^+) \tag{3}$$

are introduced and the state vector is denoted by $\mathbf{x}_j \coloneqq [t_j, x_j, \dot{x}_j^+, \dot{y}_j^+]^{\mathrm{T}}$.

Modelling the drill system as a *time-discrete* dynamic system results in a set of four *difference equations* which are to be derived in the subsequent sections. The difference equations map the system's state at time t_j on the system's state at time t_{j+1}. Accordingly we obtain a set of nonlinear algebraic equations including case differentiation

$$\mathbf{f}(\mathbf{x}_j, \mathbf{x}_{j+1}) = \mathbf{0}, \tag{4}$$

mapping the contact state of a ball–plunger impact $\mathbf{x}_j$ onto a contact state of a ball–plunger impact $\mathbf{x}_{j+1}$. In the next two sections the difference equations are derived. In Section 2.2 the subsequent instant of time t_{j+1} is gained and in Section 2.3 the remaining state variables $x_j, \dot{x}_j^+, \dot{y}_j^+$ are obtained.

2.2. Calculation of the subsequent time of impact t_{j+1}

The motion $y(t)$ of the ball after the impact j with the plunger will be given by the initial value problem

$$\ddot{y} = -g \quad \text{with } y(t_j) = u(t_j), \quad \dot{y}(t_j) = \dot{y}_j^+ \quad \forall t \in [t_j, t_{j+1}), \tag{5}$$

where $u(t_j)$ and $\dot{y}_j^+$ are the initial displacement and the initial velocity after the ball–plunger contact, respectively. Using Eq. (1), the initial displacement is

$$u(t_j) = x(t_j) - \bar{u}(t_j) = x_j - u_0 \cos \Omega t_j. \tag{6}$$

Solving the initial value problem Eq. (5) yields the equation of motion of the ball after impact j:

$$y(t) = -\frac{g}{2}(t - t_j)^2 + \dot{y}_j^+(t - t_j) + x_j - u_0 \cos \Omega t_j \quad \forall t \in [t_j, t_{j+1}). \tag{7}$$

The motion $x(t)$ of the oscillator after the impact j is given by the initial value problem

$$\ddot{x} = -g - \frac{F_A}{M} \quad \text{with } x(t_j) = x_j, \quad \dot{x}(t_j) = \dot{x}_j^+ \quad \forall t \in [t_j, t_{j+1}), \tag{8}$$

where M denotes the oscillator's mass on which the axial preload F_A acts. Solving the initial value problem, Eq. (8) yields the equation of motion of the oscillator after impact j

$$x(t) = -\frac{g + F_A/M}{2}(t - t_j)^2 + \dot{x}_j^+(t - t_j) + x_j \quad \forall t \in [t_j, t_{j+1}). \tag{9}$$

In the next step the equations for computing the still unknown subsequent ball–plunger impact time t_{j+1} are derived. It has to be distinguished between two possible contact cases: Case 1 is given by a ball–deflector contact condition at the contact time t_{Wj}

$$\text{contact case 1:} \quad y(t_{Wj}) = 0 \quad \text{with } t_{Wj} \in (t_j, t_{j+1}) \tag{10}$$

and case 2 corresponds to a *multiple ball–plunger impact* at contact time t_{j+1}

$$\text{contact case 2:} \quad y(t_{j+1}) = u(t_{j+1}). \tag{11}$$

Besides a multiple impact at the plunger it is theoretically also possible to simulate *multiple impacts at the deflector*, if the ball moves under gravitational influence. This kind of motion corresponds to a rattling

behaviour at the deflector. Here, it can be possible for the ball to bounce infinitely often against the deflector and gets to rest at zero velocity after a finite time, and before the plunger hits the ball again. This phenomenon is rather likely to appear with zero or negative axial preload on the transducer. In the following a positive preload is assumed at which multiple deflector impacts are hardly observed in simulations and thus will be neglected.

Let us first assume that a ball–deflector impact occurs (*contact case* 1). The time of impact between the ball and the deflector, t_{Wj}, follows from Eq. (10). The contact condition results in a quadratic polynomial in $(t_{W_j} - t_j)$, which solves to

$$t_{W_j} = t_j + \frac{1}{g}\left[\dot{y}_j^+ \mp \sqrt{(\dot{y}_j^+)^2 + 2g\underbrace{(x_j - u_0\cos\Omega t_j)}_{=u(t_j)>0}}\right]. \tag{12}$$

The minus-solution is neglected, since it would yield a t_{W_j} with $t_{W_j} < t_j$, but this makes no sense in this context.

Under the assumption that a multiple impact at the plunger (*contact case* 2) occurs, i.e. a repeated contact between ball and plunger without an intermediate contact between ball and deflector, we are going to calculate the impact time t_{j+1}. The necessary condition for a plunger–ball contact is given in Eq. (11). Inserting subsequently Eqs. (1), (7) and (9) into Eq. (11) yields

$$(\dot{y}_j^+ - \dot{x}_j^+)(t_{j+1}^* - t_j) = -u_0(\cos\Omega t_{j+1}^* - \cos\Omega t_j) - \frac{F_A}{2M}(t_{j+1}^* - t_j)^2. \tag{13}$$

We have to find the smallest real t_{j+1}^* with $t_j < t_{j+1}^*$ solving Eq. (13). This task describes no trivial problem, since Eq. (13) is of transcendent type. In general, this type of problem can be stated as: "Find all points of intersection between a parabola and a cosine."

Then the calculated time t_{j+1}^* has to be compared with the time t_{W_j} which was calculated under the assumption of a deflector–ball impact. If

$$t_{W_j} < t_{j+1}^* \quad \vee \quad t_{j+1}^* \in \emptyset, \tag{14}$$

then a ball–deflector contact occurs. In any other case

$$t_{j+1}^* < t_{W_j} \tag{15}$$

holds and a multiple impact occurs at the plunger. In either case the corresponding ball–plunger impact time t_{j+1} has to be found.

The dissipated energy during impacts between ball and deflector is modelled via a coefficient of restitution

$$\alpha_2 := -\frac{\dot{y}(t_{W_j}^+)}{\dot{y}(t_{W_j}^-)}. \tag{16}$$

Computing the time derivative of $y(t)$ given in Eq. (7) and inserting $\dot{y}(t_{W_j}^-)$ into Eq. (16) yields

$$\dot{y}(t_{W_j}^+) = \alpha_2(g(t_{W_j} - t_j) - \dot{y}_j^+). \tag{17}$$

It is $\dot{y}(t_{W_j}^-) = \dot{y}(t_{W_j})$ the velocity of the ball before the impact with the deflector and $\dot{y}(t_{W_j}^+)$ the velocity of the ball after the impact with the deflector. The motion of the ball after the impact with the deflector is described by the initial value problem

$$\ddot{y}_2(t) = -g \quad \text{with } y_2(t_{W_j}) = 0, \quad \dot{y}_2(t_{W_j}) = \dot{y}(t_{W_j}^+), \quad t \in [t_{W_j}, t_{j+1}) \tag{18}$$

with the solution

$$y_2(t) = -\frac{g}{2}(t - t_{W_j})^2 + \dot{y}(t_{W_j}^+)(t - t_{W_j}). \tag{19}$$

The necessary condition to compute the contact time t_{j+1} between plunger and ball is

$$y_2(t_{j+1}) = u(t_{j+1}). \tag{20}$$

Substituting $y_2(t)$ given in Eq. (19) and $u(t)$ given in Eq. (1) into Eq. (20) again yields a transcendent equation in t_{j+1}, i.e. again real numbers of intersections between a cosine and a parabola have to be determined. The smallest real number t_{j+1} with $t_{W_j} < t_{j+1}$ is the sought time of impact. If it does not exist the rare case of a multiple impact at the deflector occurs.

2.3. Calculation of the remaining state variables

In the preceding subsection the impact time t_{j+1} at which the ball rebounds off the plunger was determined for both possible cases of a plunger–plunger multiple impact and a plunger–deflector–plunger impact. For the complete definition of the systems state, the calculation of the three remaining state variables is still missing. These are the departure velocity $\dot{y}^+_{j+1}$ of the ball after the impact at the plunger, the oscillator's velocity $\dot{x}^+_{j+1}$ after the impact and the displacement x_{j+1} of the oscillator and the ball at impact, respectively.

For a kinematic description of the impact at the plunger the coefficient of restitution

$$\alpha_1 := -\frac{v^+_{\text{ball}} - v^+_{\text{plunger}}}{v^-_{\text{ball}} - v^-_{\text{plunger}}} = -\frac{\dot{y}^+_{j+1} - \dot{u}^+_{j+1}}{\dot{y}_2(t_{j+1}) - \dot{u}(t_{j+1})} \tag{21}$$

is introduced. Conservation of momentum yields a second equation for the two sought velocities

$$m \cdot v^-_{\text{ball}} + M \cdot v^-_{\text{oscillator}} = m \cdot v^+_{\text{ball}} + M \cdot v^+_{\text{oscillator}}$$

or with the short notation

$$m \cdot \dot{y}_{(2)}(t_{j+1}) + M \cdot \dot{x}(t_{j+1}) = m \cdot \dot{y}^+_{j+1} + M \cdot \dot{x}^+_{j+1}, \tag{22}$$

where m and M in Eq. (22) are the mass of the ball and the oscillator, respectively. The ball's velocity before the impact v^-_{ball} is obtained in the case of a multiple impact by $\dot{y}(t_{j+1})$ and in the case of an impact with the deflector it is obtained by $\dot{y}_2(t_{j+1})$.

Note further that the ball's mass m only appears in the conservation of momentum Eq. (22) and does not influence its equation of free motion Eq. (5). However, the oscillator's mass M is included in its equation of motion Eq. (8) in the case that the axial preload F_A exists.

Introducing the ratio of masses

$$\mu := \frac{M}{m} \tag{23}$$

the two Eqs. (21) and (22) which linearly depend on the sought velocities are reorganised with respect to the velocities:

$$\dot{x}^+_{j+1} = \frac{1}{1+\mu}[(1+\alpha_1)(\dot{y}_{(2)}(t_{j+1}) + \dot{\bar{u}}(t_{j+1})) + (\mu - \alpha_1)\dot{x}(t_{j+1})], \tag{24}$$

$$\dot{y}^+_{j+1} = \frac{1}{1+\mu}[\mu(1+\alpha_1)(\dot{x}(t_{j+1}) - \dot{\bar{u}}(t_{j+1})) - (\mu\alpha_1 - 1)\dot{y}_{(2)}(t_{j+1})]. \tag{25}$$

Finally, the oscillator's displacement during impact time is obtained by substituting t_{j+1} into the equation of motion for $x(t)$, compare Eq. (9)

$$x_{j+1} = x(t_{j+1}) = -\frac{g + F_A/M}{2}(t_{j+1} - t_j)^2 + \dot{x}^+_j(t_{j+1} - t_j) + x_j. \tag{26}$$

2.4. Summary of the contact-impact model

The model parameters are α_1, α_2, μ and M, which are the coefficient of restitution between impacting mass and the oscillator tip, the coefficient of restitution between impacting mass and deflector, the mass ratio between the mass of the oscillator and the impacting mass, and the oscillator's mass, respectively. The process parameters are u_0, Ω and $F_A(t)$, corresponding to the amplitude of the oscillator tip, the circular excitation frequency of the oscillator and the axial preload, respectively. The model's discrete state variables are the time

of impact t_j, the oscillator displacement x_j at the time of impact, the velocity $\dot{x}_j^+$ of the oscillator immediately after the impact and the velocity of the impacting mass $\dot{y}_j^+$ immediately after the impact.

Beginning with a state $\mathbf{x}_j = [t_j, x_j, \dot{x}_j^+, \dot{y}_j^+]^{\mathrm{T}}$ at a contact between ball (which is the impacting mass) and plunger (which is the oscillator tip), the mapping from state j to state $j+1$ is given as an implicit function

$$\mathbf{f}(\mathbf{x}_j, \mathbf{x}_{j+1}) = \mathbf{0} \tag{27}$$

composed of Eqs. (12), (13), (14), (20) and (24)–(26). The computation of $\mathbf{x}_{j+1}$ is split into two steps. In the first step the contact time t_{j+1} is determined. In the second step the remaining state quantities, $x_{j+1}, \dot{x}_{j+1}^+, \dot{y}_{j+1}^+$ can be computed. To determine the contact time t_{j+1}, it must be distinguished between a single or a multiple ball–plunger impact. To do so, two time instants are computed and compared. This is on the one hand the time

$$t_{W_j} = t_j + \frac{1}{g}\left[\dot{y}_j^+ + \sqrt{(\dot{y}_j^+)^2 + 2g(x_j - u_0 \cos \Omega t_j)}\right], \tag{28}$$

given in Eq. (12), which contains the duration until a contact between ball and deflector occurs. On the other hand it must be checked whether a multiple impact between ball and plunger may occur *before* the next ball–deflector contact could take place. Therefore, the time instant t_{j+1}^* must be computed by solving

$$(\dot{y}_j^+ - \dot{x}_j^+)(t_{j+1}^* - t_j) = -u_0(\cos \Omega t_{j+1}^* - \cos \Omega t_j) - \frac{F_A}{2M}(t_{j+1}^* - t_j)^2, \tag{29}$$

as stated in Eq. (13). According to the contact condition given in Eq. (14) both time instants are compared: the case that a ball–plunger contact is followed by a ball–deflector contact is described by Eq. (14):

$$t_{W_j} < t_{j+1}^* \vee t_{j+1}^* \in \emptyset \;\Rightarrow\; t_{j+1} = t^{**}. \tag{30}$$

Thus, the subsequent time instant t_{j+1} for the next ball–plunger contact is obtained by solving Eq. (20):

$$-\frac{g}{2}(t^{**} - t_{W_j})^2 + \dot{y}(t_{W_j}^+)(t^{**} - t_{W_j}) = x_j - u_0 \cos \Omega t^{**}. \tag{31}$$

Contrary, in case that a multiple ball–plunger contact occurs, i.e. two successive ball–plunger contacts occur without a ball–deflector contact in-between, the corresponding instant of time is given by Eq. (15):

$$t_{W_j} > t_{j+1}^* \;\Rightarrow\; t_{j+1} = t_{j+1}^*. \tag{32}$$

Now, with the known discrete state t_{j+1}, in the second step the remaining discrete states follow in an explicit manner from Eqs. (24)–(26)

$$\dot{x}_{j+1}^+ = \frac{1}{1+\mu}[(1+\alpha_1)(\dot{y}_{(2)}(t_{j+1}) + \dot{u}(t_{j+1})) + (\mu - \alpha_1)\dot{x}(t_{j+1})], \tag{33}$$

$$\dot{y}_{j+1}^+ = \frac{1}{1+\mu}[\mu(1+\alpha_1)(\dot{x}(t_{j+1}) - \dot{u}(t_{j+1})) - (\mu\alpha_1 - 1)\dot{y}_{(2)}(t_{j+1})], \tag{34}$$

$$x_{j+1} = -\frac{g + \dfrac{F_A}{M}}{2}(t_{j+1} - t_j)^2 + \dot{x}_j^+(t_{j+1} - t_j) + x_j. \tag{35}$$

The result of this procedure is the state vector $\mathbf{x}_{j+1}$.

3. Analysing the vibro-impact system by applying set-oriented techniques

In order to obtain an impression on the dynamical behaviour of the system components, one possibility is to look at a time series representation of the displacements. As an example we use the following system parameters: $u_0 = 10\,\mu\mathrm{m}$, $\Omega = 2\pi \cdot f = 2\pi \cdot 20\,\mathrm{kHz} = 4\pi 10^4\,\mathrm{s}^{-1}$, $\mu = 200$, $\alpha_1 = 0.9$, $\alpha_2 = 0.7$, $F_A \cdot M = 10\,\mathrm{m/s^2}$, $g = 9.81\,\mathrm{m/s^2}$. As initial conditions for the state space variables $t_0 = 0\,\mathrm{s}$, $\dot{y}_0^+ = -0.001\,\mathrm{m/s}$, $x_0 = 0.001\,\mathrm{m}$ and $\dot{x}_0^+ = 0\,\mathrm{m/s}$ were used. Then $x(t)$, $y(t)$ and $u(t)$ were determined by iteratively applying the map given in Eqs. (27)–(35) and using the solutions Eqs. (7), (9) and (19) of the initial value problems between every two impact times. Fig. 4 graphs the results for a simulation time of 55 ms. The oscillator—released at $t_0 = 0$ at an

initial height of $x_0 = 1\,\text{mm}$—moves in the first instance under gravitational force and preload towards the deflector. This leads to an increase of the ball's bouncing frequency which accomplishes to keep the oscillator at a level of $x(t) = 0.2\,\text{mm}$ for $10\,\text{ms} < t < 11\,\text{ms}$.Fig. 5 enlarges this situation. Here, multiple impacts at the oscillator can be observed at $t = 9.2\,\text{ms}$ (see detail in Fig. 6) and $t = 10.6\,\text{ms}$. As time increases beyond $t = 11\,\text{ms}$ the oscillator–ball impacts transmit enough momentum to the oscillator to raise it to a level of $x(t = 45\,\text{ms}) = 2.3\,\text{mm}$ as can be seen in Fig. 4. Fig. 7 shows the time series solution for a simulation length of approx. 0.5 s. As it could be observed in laboratory experiments with a prototype of the USDC an irregular motion of the ball and the oscillator is revealed. This refers to a chaotic nature of the time discrete system map.

3.1. The set-oriented method

In the model based design of deterministic nonlinear dynamical systems it may be important to obtain information about their global long-time behaviour. This may include the detection of equilibrium points, periodic or chaotic solutions as well as their basins of attraction. Classic analysis approaches like equivalent

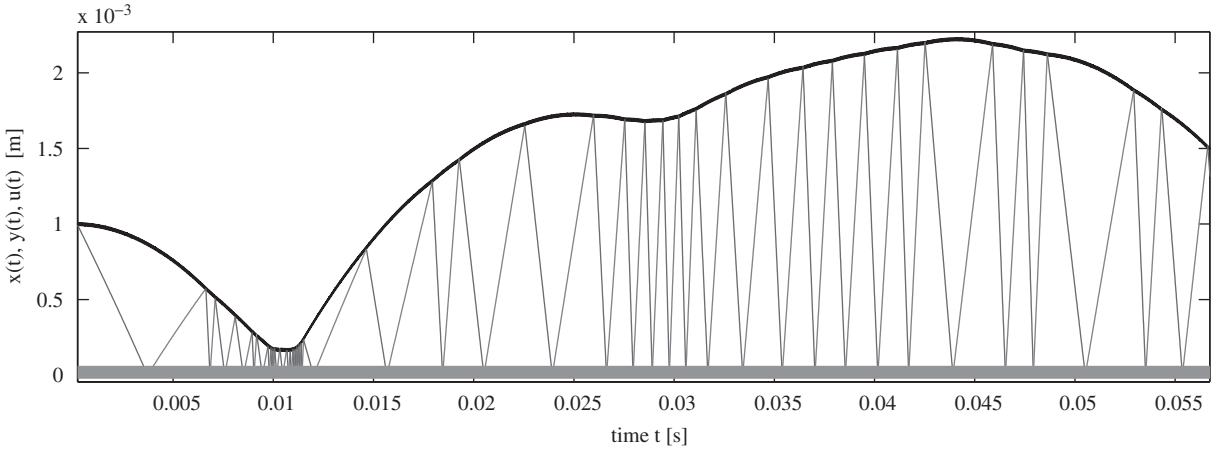

Fig. 4. Time series for first 55 ms of oscillator $x(t)$ (dark curve) and ball $y(t)$ (light grey parabolae) displacements.

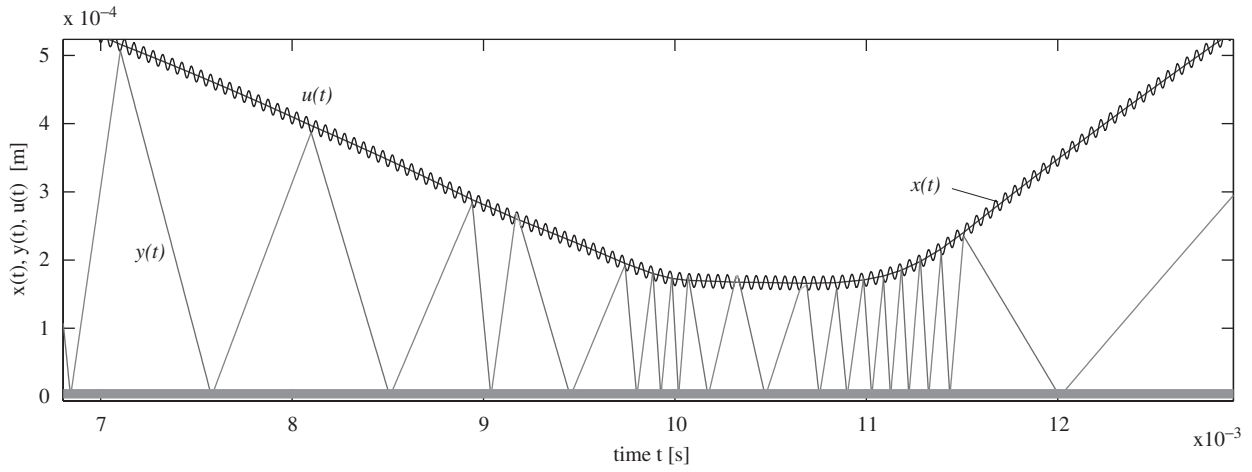

Fig. 5. Time series detail around $t = 10\,\text{ms}$ of oscillator $x(t)$ and ball $y(t)$ displacements. At the provided resolution the harmonic oscillation of the plunger $u(t)$ is also visible here.

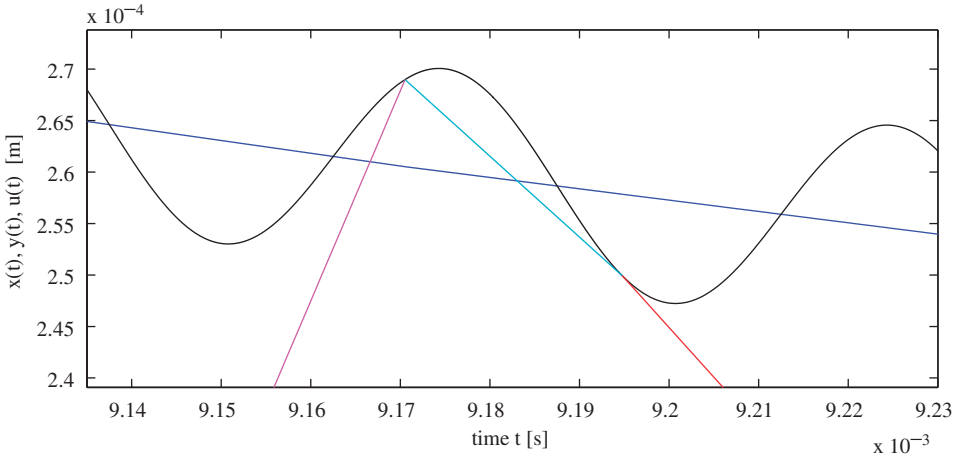

Fig. 6. A multiple impact at the plunger: detail of Fig. 5 around 9.17 ms.

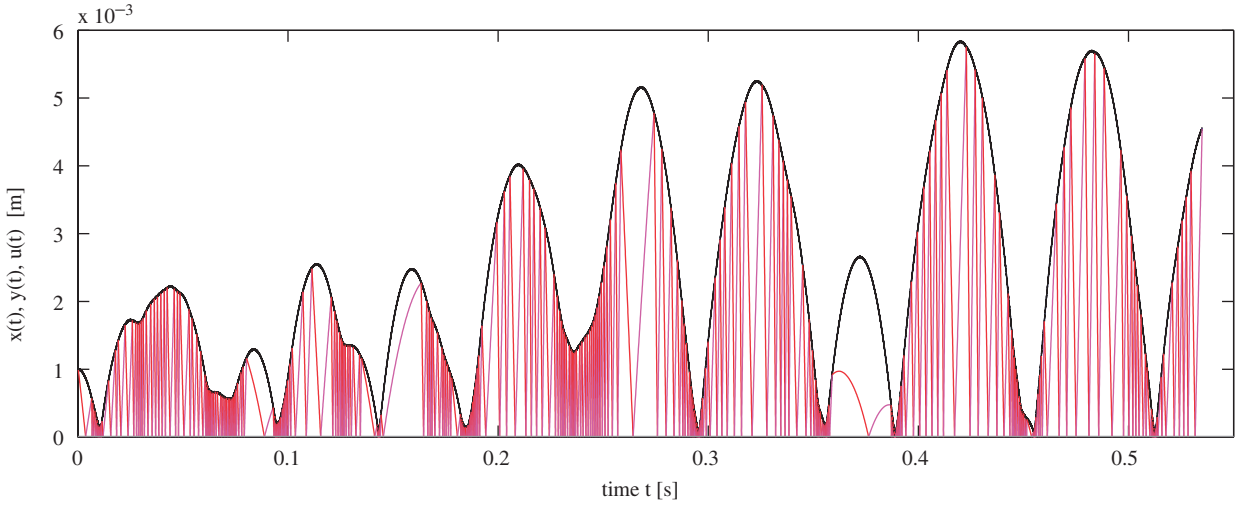

Fig. 7. Time series for first 550 ms of oscillator $x(t)$ (upper envelope, dark curve) and ball $y(t)$ (lower trajectory parabolae) displacements.

linearisation or continuation methods are not applicable in case the dynamical system shows chaotic behaviour. Also, in dynamic systems having low damping, as it is the case for example in many vibro-impact systems, the determination of periodic solutions may be difficult.

From a topological point of view, equilibrium points as well as periodic or chaotic solutions are classified as invariant sets. Thus, they depend on system parameters only and are invariant with respect to time. At this point it is helpful to introduce the concept of an *attractor*. An attractor or an attracting set describes that part or subset of a phase space, towards which the systems dynamics will eventually evolve. With evolution in time, an attractor is an invariant set. That is, once the systems state is *on* the attractor, it will never again leave this part of its phase space under the influence of the underlying dynamics. Thus, to find attractors is an essential way in characterising the long-term behaviour of a dynamical system.

Assume, the dynamical system under investigation can be explicitely stated in the form

$$\mathbf{x}_{j+1} = \mathbf{T}(\mathbf{x}_j), \quad j = 0, 1, 2, \ldots, \quad \mathbf{T} : \mathbb{R}^n \mapsto \mathbb{R}^n \tag{36}$$

with an initial state $\mathbf{x}_0 \in \mathbb{R}^n$ where $\mathbf{x}_j = \mathbf{x}(t_j)$ describes the system's state at time step t_j. In the case of Section 2.4 $\mathbf{T}$ describes the numerical solution of Eq. (27).

Considering the map $\mathbf{T}$, the definitions of an invariant set and an attractor can be stated, see Ref. [5]:

- A subset $\mathscr{A} \subset \mathbb{R}^n$ is called *invariant*, if $\mathbf{T}(\mathscr{A}) = \mathbf{T}^{-1}(\mathscr{A}) = \mathscr{A}$.
- If there exists a *basin of attraction* $\mathscr{D}_\mathscr{A}$ with $\mathscr{A} \subset \mathscr{D}_\mathscr{A}$ and $\mathscr{D}_\mathscr{A} \subset \mathbb{R}^n$ then $\mathscr{A}$ is called an *attractor*. If $\mathscr{D}_\mathscr{A} = \mathbb{R}^n$, then $\mathscr{A}$ is called a *global attractor*.

However, for the determination of an attractor, for obvious reasons it is not possible to treat the entire $\mathbb{R}^n$ numerically. Instead one has to limit the state space under investigation to a subset of interest, which is called $Q \subset \mathbb{R}^n$. Here with the so called *relative global attractor*, denoted by $\mathscr{A}_Q$, can be introduced (see also Refs. [9,5]): $\mathscr{A}_Q$—the global attractor *relative* to some given set Q of interest—is defined as the intersection of all forward images of Q, or

$$\mathscr{A}_Q(\mathbf{T}) := \bigcap_{k=0}^{\infty} \mathbf{T}^k(Q). \tag{37}$$

3.2. Approximating the relative global attractor

This section is going to show how the relative global attractor of some given time-discrete dynamical system $\mathbf{T}$ can be numerically found. Here, the idea behind the set-oriented approach which gives the basis for the set-oriented numerical methods will be introduced. The aim is to approximately cover the attractor with a set of small rectangular (n-dimensional) boxes. In case of the model suggested in this paper, $n = 4$. The first step is the choice of a rectangular subset Q of the underlying phase space $\mathbb{R}^n$. The dynamics of the system will only be analysed within this subset. If the analysis has to be started without any a priori knowledge of the system, it is recommended to choose a rather large section of the phase space. Next, a *box subdivision algorithm* [9,10] is applied. It consists of two steps which are iteratively repeated a finite number of times. The rectangular subset $Q^{(0)} = Q$ is the initial box to begin with. The two steps are:

(1) *Subdivision*: Given the ith subdivision iteration step with $N^{(i)}$ boxes $\mathscr{B}_k^{(i)}$, $k = 1, \ldots, N^{(i)}$, and

$$\bigcup_{k=1}^{N^{(i)}} \mathscr{B}_k^{(i)} = Q^{(i)} \subseteq Q^{(0)} \subset \mathbb{R}^n. \tag{38}$$

At the next subdivision iteration step $i+1$ bisect each box $\mathscr{B}_k^{(i)}$ into two smaller boxes of same size using hyperplanes $\mathscr{P} \subset \mathbb{R}^{n-1}$. This results in $2N^{(i)}$ boxes with $\bigcup_{k=1}^{2N^{(i)}} \mathscr{B}_k^{(i+1)} = Q^{(i)}$.

(2) *Selection*: Determine the preimage $\mathbf{T}^{-1}(\mathscr{B}_k^{(i+1)})$, $k = 1, \ldots, 2N^{(i)}$ of each of the refined boxes by applying the inverted map. Then discard those boxes $\mathscr{B}_k^{(i+1)}$, whose preimage does *not* intersect with the current collection of boxes.[1] Thus, the subset $Q^{(i+1)}$ of the next iterative step $i+1$ follows from the remaining boxes.

For the bisection of the current boxes $\mathscr{B}_k^{(i)}$ during the subdivision step the cutting direction is cyclic permuted along the n dimensions of the phase space. The algorithms for global numerical analysis of dynamical systems described above have been implemented in a software package called *Global Analysis of Invariant Objects* (GAIO) [9].

[1]The existence of the inverted map $\mathbf{T}^{-1}$ is in practice not required. The selection of those refined boxes, which will be discarded, is done in such a way, that *forward*-images are determined of each box. Then those boxes are discarded which do not intersect with any of the images.

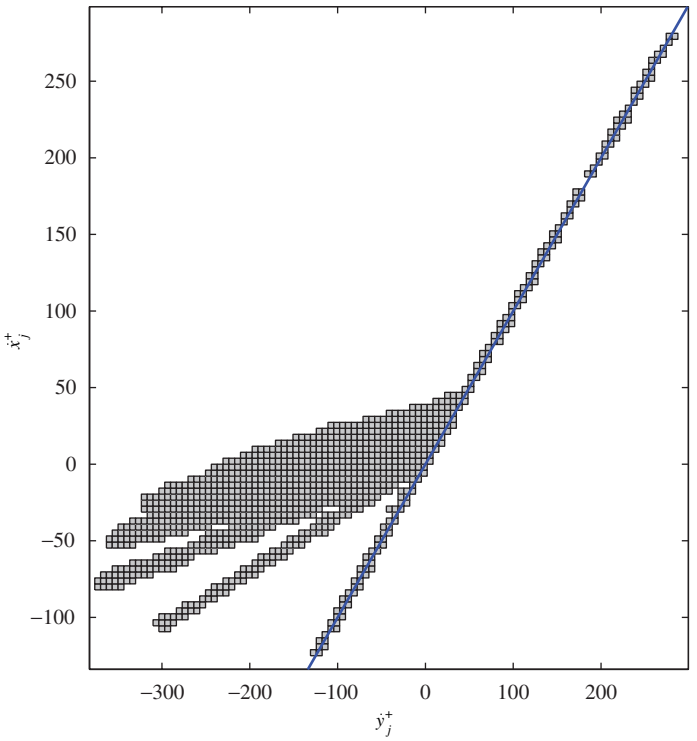

Fig. 8. Relative global attractor $\mathscr{A}_Q$ approximated by a box covering projected on $\dot{y}$–$\dot{x}$-plane.

3.3. Relative global attractors of the vibro-impact system

Applying the set-oriented technique to the four-dimensional state space of the model derived in this paper yields information on the system's global dynamics. For one set of parameters the computation was applied to the model. Fig. 8 shows a projection of the resulting four-dimensional box-approximated attractor on the $\dot{y}$–$\dot{x}$-plane. Long-term trajectories in phase-space or time series analysis in the case of a non-smooth system like the one under consideration could not reveal dynamical features and properties of the system. As a particular information extracted from this view, it can be gained that only a limited range of velocities can occur during the chaotic type of motion as it is covered by boxes in Fig. 8. A straight diagonal line in the figure indicates states with $\dot{y}_j = \dot{x}_j$. No states can exist on the lower right-hand side of this line, otherwise penetration between ball and plunger would happen. It is apparent that most possible states appear in the range of negative velocities $\dot{x}$. This means, during most impacts the oscillator is about to move towards the deflector. It is possible to compute a numerical estimate for the mean momentum which gets transfered from the oscillator to the free mass. In this way we can evaluate the quality of the specific set of parameters with which this calculation has been performed. Fig. 9 shows a projection of the relative global attractor projected into the $\dot{y}$–x–$\dot{x}$-space. Again the border beyond which penetration would be violated is included as a tilted plane. From the three-dimensional view one can deduce that high velocities of the ball do only occur at very small displacements of the oscillator, i.e. only if the gap between plunger and deflector is very small.

Summarising these results it is possible to determine, which possible states the system can accept during its long-term behaviour *without* any long-term integration of the map which can be erroneous.

4. Outlook

The efficiency of the method encourages further analysis. Analysing the model for a large set of parameter combinations shall reveal the nature of the underlying dynamics, and shall indicate whether the performance

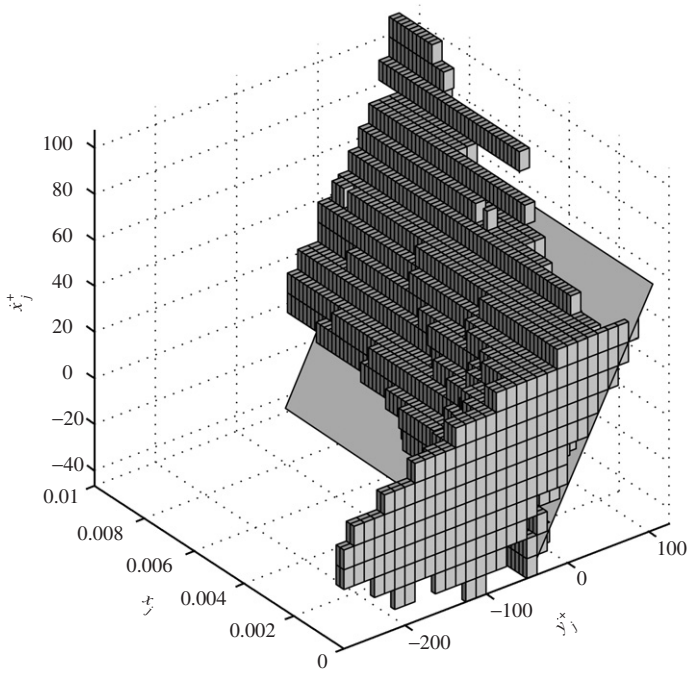

Fig. 9. Relative global attractor $\mathscr{A}_Q$ approximated by a box covering projected into $\dot{y}$–x–$\dot{x}$-space.

of a scaling up of the drill's dimensions is technologically feasible. Therefore, statistical measures based on the energy transfer from the piezoelectric actuator to the drill stem must be defined and combined with a material removal model. Furthermore, the modification of the GAIO tool [9] to determine basins of attraction is important to evaluate the robustness of operation of the drilling device. Beyond the theoretical work a comparison of measured time series data with the simulated data is planned, e.g. by determining correlation coefficients of chaotic time series.

Acknowledgments

We thank the German Research Foundation (DFG) and PaSCo (Paderborn Institute for Scientific Computation) for their kind support of this research project.

References

[1] Y. Bar-Cohen, S. Sherrit, B. Dolgin, N. Bridges, X. Bao, Z. Chang, A. Yen, R. Saunders, Ultrasonic/Sonic Driller/Corer (USDC) as a sampler for planetary exploration, *2001 IEEE Aerospace Conference on the Topic of "Missions, Systems and Instruments for In Situ Sensing,"* Big Sky, Montana, March 10–17, 2001.

[2] M. Badescu, X., Bao, Y. Bar-Cohen, Z. Chang, S., Sherrit, Integrated modeling of the ultrasonic/sonic drill/corer—procedure and analysis results. *Proceedings to SPIE Smart Structures and Integrated Systems Conference*, Vol. 5764-37, SPIE, San Diego, CA, March 7–10, 2005.

[3] N. Neumann, T. Sattel, J. Wallaschek, On the analysis of a simple impact drill model using set-oriented numerical methods, *Proceedings in Applied Mathematics and Mechanics, PAMM* 5 (1) (2005) 119–120.

[4] N. Neumann, T. Sattel, On the modelling and model analysis of a piezoelectric impact drilling device, *Proceedings of Fifth EUROMECH Nonlinear Dynamics Conference* (*ENOC*), Eindhoven, 2005.

[5] M. Dellnitz, O. Junge, Set oriented numerical methods for dynamical systems, in: B. Fiedler, G. Iooss, N. Kopell (Eds.), *Handbook of Dynamical Systems III*, World Scientific, Singapore, 2002.

[6] C.S. Hsu, A generalized theory of cell-to-cell mapping for nonlinear dynamical systems, *ASME, Transactions, Journal of Applied Mechanics* 48 (1981) 634–642
C.S. Hsu, *Winter Annual Meeting*, American Society of Mechanical Engineers, Washington, DC, November 15–20, 1981.

[7] V.I. Babitsky, *Theory of Vibro-Impact Systems and Applications*, Springer, Berlin, 1998.

[8] R.I. Leine, H. Nijmeijer, Dynamics and bifurcations in non-smooth mechanical systems, *Lecture Notes in Applied and Computational Mechanics*, Vol. 18, Springer, Berlin, Heidelberg, New York, 2004.
[9] M. Dellnitz, G. Froyland, O. Junge, The algorithms behind GAIO—set oriented numerical methods for dynamical systems, in: B. Fiedler (Ed.), *Ergodic Theory, Analysis, and Efficient Simulation of Dynamical Systems*, Springer, Berlin, 2001, pp. 145–174.
[10] M. Dellnitz, A. Hohmann, A subdivision algorithm for the computation of unstable manifolds and global attractors, *Numerische Mathematik* 75 (1997) 293–317.